THEO
CHEM

The chemical nature of very strong hydrogen bonds in some categories of compounds

A.H. Pakiari *, K. Eskandari

Chemistry Department, College of Sciences, Shiraz University, Shiraz 71454, Iran

Abstract

In the current research, chemical nature of very strong hydrogen bonds in their three fundamental cases, resonance assisted hydrogen bond [RAHB], negative charge assisted hydrogen bond [(−)CAHB], and positive charge assisted hydrogen bond [(+)CAHB] is studied. The results are obtained at B3LYP/6-311++G** and MP2/6-311++G** level of theories. Attention is focused on topological parameters such as electron density, its Laplacian, kinetic energy density, potential energy density and energy density at the bond critical points (BCP) of O···H and O–H bonds from Bader's atoms in molecules (AIM) theory. Charge transfer energies based on natural bond orbital (NBO) analysis are also considered. Our results show that these hydrogen bonds are partially electrostatic and partially covalent in nature, in which the covalent contribution increases as the stabilization energy of hydrogen bond increases. In addition, it is shown that, as the O–H–O angle in intramolecular hydrogen bonds approaches to 180°, the charge transfer energy from oxygen lone pairs to antibonding NBO of O–H increases. In the investigated systems, double minimum no barrier (DM/NB) potential energy surface (PES) is obtained for hydrogen transfer between the two oxygens. AIM analysis based on DFT calculation for the transition states (TSs) show that the hydrogen atom is connected to the oxygens with two almost identical covalent bonds with some contribution of electrostatic interaction, while MP2 calculation predict two covalent O–H bonds in some cases.
© 2005 Elsevier B.V. All rights reserved.

Keywords: RAHB; (+)CAHB; (−)CAHB; Nature of chemical bond

1. Introduction

After suggestion of hydrogen bond by Huggins [1], Latimer and Rodebush [2], and then cited by Lewis's 1923 book on valance theory [3] as 'Bivalent Hydrogen', many books [4–9], reviews [10,11], and various articles appeared about H-bonding. Recently, many researches are devoted to very strong hydrogen bonds, because of their important role in biochemical reactions, and enzyme catalysis as transition state [12–15]. What makes them to be distinguished form ordinary hydrogen bonds is their unusual stabilization energy. These types of hydrogen bonds have been widely studied, both experimentally and theoretically [16–28]. Gilli classified all cases of strong and very strong hydrogen bonds to three fundamental types: negative charge assisted hydrogen bond [(−)CAHB], positive charge assisted hydrogen bond [(+)CAHB], and resonance assisted hydrogen bond [RAHB],

where the H-bond donor and acceptor atoms are connected through π-conjugated double bonds [19]. Also, Hibbert and Emsley [29] classified hydrogen bonds according to their shape of potential energy surface (PES), the energy of transition state (TS) for hydrogen transfer between two oxygens, and the O–H zero point vibrational energy (ZPE$_{O-H}$). With respect to this classification, very strong hydrogen bonds have a barrier less than (or near to) ZPE$_{O-H}$ [12].

Experimental works show that very strong hydrogen bonds always have unusual downfield ^{1}H NMR chemical shifts ($\delta_H =$ 16–20 ppm) with their proton highly deshielded [17]. On the other hand, it has been shown that shortening of the O···O distance, in O–H···O systems, is associated with a decrease of IR v(O–H) stretching frequencies up to 2560 cm^{-1} [16,17]. Although, ordinary hydrogen bonds are believed to be electrostatic in nature [8], Gilli et al. proposed that these strong hydrogen bonds have significant covalent character [19]. Larsen et al. studied benzoylaceton with X-ray and neutron diffraction [30]; they concluded that the hydrogen bond in this molecule is partially covalent and partially electrostatic. Using a DFT calculation, Iversen et al. showed that the covalency is important in the RAHB system in the benzoylaceton [31].

* Corresponding author. Tel.: +98 711 2273900; fax: +98 711 2286008.
E-mail address: pakiari@susc.ac.ir (A.H. Pakiari).

In the current research, the nature of very strong hydrogen bond in its three different cases were examined, in their minima and transition state structures. Attention was focused on electron densities, $\rho(r)$, and its corresponding Laplacian, kinetic energy density, $G(r)$, potential energy density, $V(r)$, and the energy density, $H(r)$, from Bader's atoms in molecules (AIM) theory [32]. In addition, the natural bond orbital (NBO) analysis [33,34] was carried out to get more information about these hydrogen bonds.

2. Computational details

Molecular geometries and their electronic wave function have been optimized with Gaussian 98 [35] program, using $6\text{-}311++G^{**}$ basis set at the density functional method, with the Backe's three parameter hybrid exchange functional [36] and the LYP correlation functional [37]. In some cases, the calculations were also carried out at MP2/$6\text{-}311++G^{**}$ level to confirm the DFT results. The NBO program, implemented in Gaussian 98 package, was used to obtain charge transfer energies associated with the hydrogen bonds [38]. Bader's theory of atoms in molecules [32] was applied to get more details about the nature of hydrogen bonds in the investigated systems. AIM2000 package [39] was used to find bond critical points.

3. Results and discussions

The results of calculations on different systems are presented in the following sections. It should be maintained that the reported values are at B3LYP/$6\text{-}311++G^{**}$ level, unless the method is given.

3.1. Hydrogen bonds in β-diketone enols

Over the years, β-diketones have been of constant interest to all fields of chemistry. Their keto–enol equilibrium, and the structure of both keto and enol forms, have been widely studied. In addition, the fact that their enol forms with cis and trans conformers are stabilized by an unusual intramolecular, and intermolecular hydrogen bonds [40], makes them still more interesting. By introducing RAHB model, Gilli et al. illustrated the role of π-delocalization in unusual nature of H-bonds in β-diketone enols and similar compounds.

First, let us compare H-bonds in different conformers of 3-hydroxypropenal (**1a** and **1b** in Fig. 1). The stabilization energy related to intermolecular H-bonds is easily calculated as a difference between the energy of the complex and the energies of isolated molecules; which gives rise to $\Delta E_{HB} = 11.32$ kcal/mol for **1a**. The situation for intramolecular H-bonds (e.g. **1b**) is not clear, because finding two structures that differ only in an H-bond, while the other effects remain
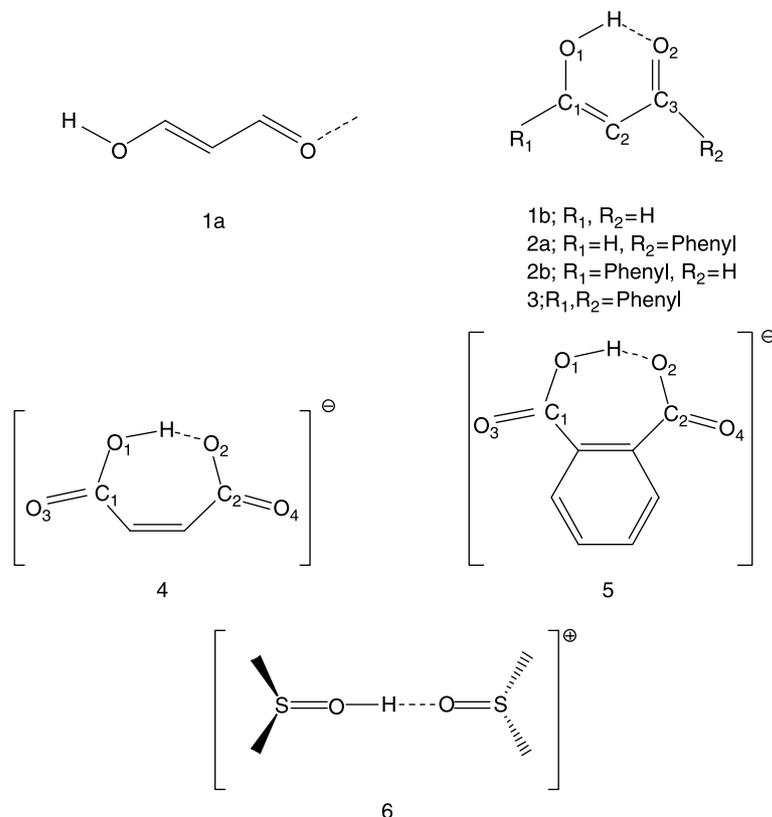
Fig. 1. Intermolecular hydrogen bond in 3-hydroxypropenal (**1a**), and intramolecular hydrogen bond which is classified as RAHB (**1b**, **2a**, **2b**, and **3**), ($-$)CAHB (**4**, **5**) and ($+$)CAHB (**6**).
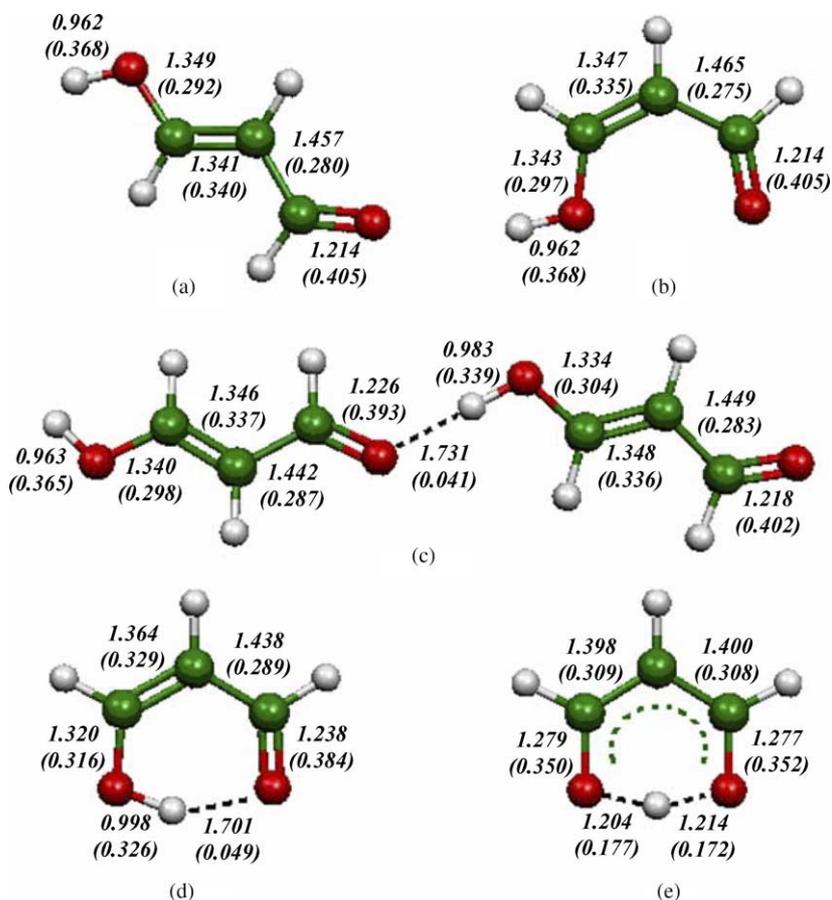
Fig. 2. Optimized geometries of *trans*−3-hydroxypropenal (a), open form of *cis*-3-hydroxypropenal (b), dimmer of *trans*−3-hydroxypropenal with an intermolecular H-bond (c), closed form of *cis*-3-hydroxypropenal with an intramolecular H-bond (d), and its TS (e), at B3LYP/6-311++G** level of theory. Distances are in Angstrom. The numbers in parentheses are electron density in atomic units.

identical, is impossible. Several ways have been suggested to estimate an intramolecular H-bond energy. One of these ways is the calculation of the difference between open and closed (or bridged) configurations (Fig. 2b and d). Using this method, a larger H-bond energy has been obtained for **1b** (13.1 kcal/mol), in comparison with **1a**. However, in this way the existence of other effects that stabilize or unstabilize the molecule might be mixed with the H-bond energy [41,42].

Two other ways, to characterize the H-bond interaction, are NBO and AIM analysis that interpret the H-bond in terms of charge transfer, and bond critical point (BCP), respectively. In Weinhold's NBO procedure, charge transfer stabilization energy (ΔE_{CT}) is proportional to the H-bond strength [43]. Furthermore, for conjugated systems, the 'charge transfer' phenomenon can be used as a criterion to obtain how the π-system is delocalized over the entire molecule [44].

NBO analysis for **1a** and **1b** shows that, the two lone pairs of the oxygen atom, have been contributed in the H-bond, Table 1, with unequal contributions due to their different orientation with respect to σ^*_{O-H}, Fig. 3. There is stronger H-bond in **1b** than **1a** because of more total charge transfer energy associated with the H-bond, and therefore, more σ^*_{O-H} occupancy in **1b**. While, co-linearity of donor–acceptor orbitals strengthened the H-bond [44], stronger H-bond is

expected for **1a**. In these systems, π-delocalization effect also plays an important role [23] that is why the H-bond is stronger in **1b** than **1a**. In order to show there is stronger π-delocalization in cis than trans, the associated charge transfer energies was compared for those without H-bond (i.e. open structure for cis, and monomer for trans). The sum of charge transfer energies between lone pairs and π electrons is 110 kcal/mol for **1a**, while it is 197 kcal/mol for **1b**.

In agreement with NBO charge transfer energies for H-bonds, the electron density values at BCP of O···H bonds are 0.041 and 0.049 a.u. for **1a** and **1b**, respectively. This also confirms that H-bond in **1b** is stronger than **1a**. Electron densities at different BCPs have been inspected for both cis and trans systems, with and without H-bond, Fig. 2. As the H-bond forms, further electron delocalization takes place.

Table 1
Charge transfer stabilization energies and occupancies of NBOs responsible for H-bond (B3LYP/6-311++G**)

	ΔE_{CT}			Occupancy		
	$n_{1O} \rightarrow \sigma^*_{O-H}$	$n_{2O} \rightarrow \sigma^*_{O-H}$	Sum	n_{1O}	n_{2O}	σ^*_{O-H}
1a	15.44	5.61	21.05	1.87501	1.9699	0.04739
1b	20.47	3.39	23.86	1.86502	1.97606	0.06332
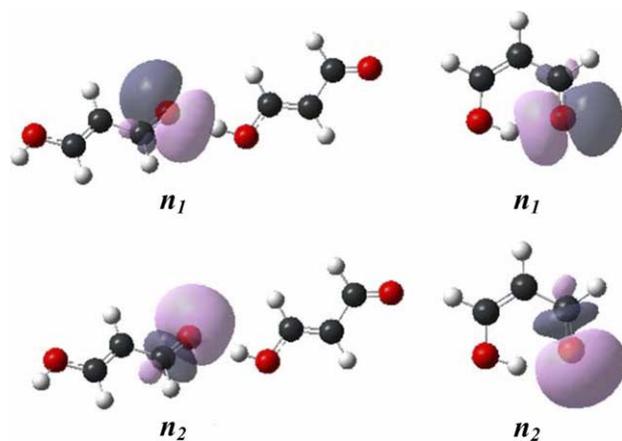
Fig. 3. Oxygen lone pairs for **1a** (left) and **1b** (right) from NBO analysis.

Consequently, O_1–H and double bonds weakens (increase in bond length with decrease in density at their BCP), while other bonds strengthen.

As it has been well discussed about unusual strength of the H-bond in **1a** and **1b** in comparison with ordinary H-bonds, it seems that, they have differences in their bond nature too. Now, we are in position to introduce some AIM parameters that properly describe bond nature. Laplacian of $\rho(r)$ is related to the bond interaction energy by a local expression of the virial theorem [32]:

$$\left(\frac{\hbar^2}{4m}\right)\nabla^2\rho(r) = 2G(r) + V(r) \qquad (1)$$

where $G(r)$ is the electronic kinetic energy density, which is always positive, and $V(r)$ is the electronic potential energy density and must be negative [45]. The sign of $\nabla^2\rho(r)$ at a BCP is determined by which energy is in excess over the virial average of 2:1 of kinetics to potential energy. A negative $\nabla^2\rho(r)$, shows the excess potential energy at BCP. It means that electronic charge is concentrated in the inter-nuclear region, and therefore, shared by two nuclei. This is the case in all shared electron (covalent) interactions. A positive $\nabla^2\rho(r)$ at a BCP reveals that the kinetic energy contribution is greater than that of potential energy, and shows depletion of electronic charge along the bond path. This is the case in all closed shell (electrostatic) interactions [32].

The electronic energy density $H(r)$ at BCP is given by [46]:

$$H(r) = G(r) + V(r) \qquad (2)$$

Bonds with covalent character must have a BCP with negative $H(r)$; but the condition in which $|V(r)| < 2G(r)$ and $|V(r)| > G(r)$, provides $\nabla^2\rho(r)$ to be positive (closed-share interaction), while $H(r)$ is negative (shared interaction). Therefore, they must be termed as partially covalent and partially electrostatic [47]. On the other hand, the cases in which the value of $|V(r)|$ is larger than $2G(r)$, and hence larger than $G(r)$, provides negative values for $\nabla^2\rho(r)$ and $H(r)$; a condition which is expected for covalent bonds. But for these cases, another criterion must be taken into account: along the bond path (BP) of covalent bonds, there must be a continuous region of space, including the

valence region of the interacting atoms, over which the Laplacian is negative [48]. If not, i.e., the valence region of atoms are separated by a region of space over which the Laplacian is positive, contribution of electrostatic (closed-shell) interaction should be considered, although both $H(r)$ and $\nabla^2\rho(r)$ are negative.

Normal hydrogen bonds are characterized as electrostatic (closed-shell) interaction; a $\rho(r)$ value at the BCP which lies within the range 0.002, 0.04 a.u. and positive values for $\nabla^2\rho(r)$ and $H(r)$ at the BCP [49]. The values of $\rho(r)$, $\nabla^2\rho(r)$, $G(r)$, $V(r)$ and $H(r)$ at the BCP of O···H in **1a** and **1b** are summarized in Table 2. The values of $\rho(r)$ and $\nabla^2\rho(r)$, classify hydrogen bond in **1a** as an ordinary (closed-shell) hydrogen bond, while a small negative value for $H(r)$ distinguishes it from an ordinary hydrogen bond. For **1b**, $\nabla^2\rho(r)$ and $H(r)$ predict it as partially covalent, with $\rho(r)$ larger than that of ordinary hydrogen bond. As a consequence, O···H in **1b** is expected to be more covalent than is in **1a**, since $H(r)_{1b}$ is more negative than $H(r)_{1a}$ [50]. Considering $H(r)$ in both **1a** and **1b** for O···H and O–H bonds, it is realized that, covalent nature of O···H bond increases as covalent nature decreases in O–H bond (Table 2).

In normal hydrogen bonds, there is a barrier for hydrogen transfer between two oxygens and the shape of PES is double minimum (DM). If this barrier is low enough (below $ZPE_{O–H}$), the hydrogen will move freely in the space between the two oxygens. This barrier lowers, as the two oxygens come closer [12]. A further shortening of the O···O distance, may remove the barrier in PES, and it makes a single minimum (SM) H-bond. Therefore, H-bonds can be categorized according to their potential barrier, in comparison with zero point energy: if the barrier is below the $ZPE_{O–H}$, it is no barrier (NB), if the barrier is approximately the same as $ZPE_{O–H}$, it is low barrier (LB), and if the barrier is above $ZPE_{O–H}$, it is called high barrier (HB). Hydrogen atom can move freely between two oxygens in NB and LB, but not for HB [23]. These nomenclatures can be useful in enzymic catalysis studies. But in the current paper, we will use additional notation for DM PESs: if zero point correction (ZPC) vanishes the barrier in DM PES, it will be called as single well (SW); otherwise, the two minima remain and the PES will be addressed as double well (DW).

The minima in the hydrogen transfer PES in **1b** are identical and a symmetric PES is expected. The barrier for proton transfer, and $ZPE_{O–H}$ (in harmonic approximation) for **1b** was 3.20 and 4.45 kcal/mol, respectively. Therefore, there is a symmetric DM/NB PES, Fig. 4. Correcting the PES with the ZPE, results a DW type PES with barrier of about 0.75 kcal/mol, which is in agreement with experimental works that confirm a DW PES for the molecule [23].

We have obtained the TS structure of the intra-molecular hydrogen transfer for **1b**, Fig. 2. The TS has a O···O separation of 2.367 Å, and the two almost identical hydrogen–oxygen separations (1.204 and 1.214 Å) indicate symmetric TS. The two C–O bond distances are also identical (1.279 and 1.277 Å) which is between a carbon–oxygen single and double bond (normal single and double C–O bonds are about 1.43 and 1.21 Å, respectively). The two carbon–carbon distances are

Table 2
The H-bond energy, NBO charge transfer energies, AIM parameters and geometries of species in their local minimum (B3LYP/6-311++G**)

Species	ΔE_{HB}	ΔE_{CT}[a]		AIM parameters at the BCP of O–H bond					AIM parameters at the BCP of O···H bond					Geometries of O–H···O part			Angle
		n_1	n_2	ρ [−1]	Lap [−2]	$G(r)$ [−1]	$V(r)$ [−1]	$H(r)$ [−1]	ρ [−2]	Lap [−1]	$G(r)$ [−2]	$V(r)$ [−2]	$H(r)$ [−2]	O–H	O···H	O···O	
1a	11.3	15.4	5.6	3.39	−2.395	6.58	−7.30	−6.65	4.06	1.31	3.47	−3.66	−0.19	0.983	1.731	2.714	178.7
1b	13.1	20.5	3.4	3.26	−2.266	6.46	−6.96	−6.31	4.86	1.35	3.99	−4.20	−0.62	0.998	1.701	2.588	145.9
2a	14.6	24.9	3.8	3.21	−2.215	6.64	−6.87	−6.20	5.51	1.45	4.57	−5.50	−0.90	1.001	1.650	2.546	146.6
2b	17.2	29.3	4.3	3.16	−2.148	6.80	−6.73	−6.05	6.01	1.48	4.92	−6.15	−1.20	1.006	1.613	2.535	150.0
3	19.1	35.2	4.6	3.10	−2.072	7.05	−6.59	−5.89	6.77	1.57	5.59	−7.20	−1.67	1.011	1.565	2.496	150.7
4	33.7[b]	104.0	9.6	2.34	−1.041	8.89	−4.38	−3.49	12.3	0.66	7.0	−15.6	−6.96	1.100	1.327	2.426	176.6
5	49.4[b]	–	–	1.82	−0.336	10.0	−2.84	−1.84	18.1	−3.32	10.0	−28.3	−18.30	1.187	1.188	2.347	178.5
6	35.2	112.7	12.1	2.12	−0.785	8.81	−3.72	−2.84	13.1	0.2	8.8	−17.0	−8.30	1.124	1.289	2.413	177.5

ΔE_{HB}, hydrogen bond energy in kcal/mol; ΔE_{CT}, charge transfer energy in kcal/mol. 'Lap' stands for $\nabla^2\rho(r)$. AIM parameters are in atomic units, distances and angles are in Angstrom and degree, respectively. [−x] means that the reported value should be multiplied by 10^{-x}.

[a] For all species charge transfers are from oxygen lone pairs (n_1 and n_2) to σ^*_{OH}, except for **5** whose donors and acceptors differ in nature.

[b] These values were extracted from linear relationship between E_{HB} and electron density at the BCP of O–H bond, Fig. 6.

also equal (1.398 and 1.400 Å), between normal carbon–carbon single and double bonds (1.54 and 1.34 Å, respectively). In agreement with RAHB model, these distances suggest π-delocalization in TS structure, which is greater than that of local minima. NBO analysis of TS structure shows that there are large charge transfer energies from C_3 lone pair to π* of both O_1–C_1 and C_3–O_2, which are 157.56 and 154.21 kcal/mol, respectively. Furthermore, the hydrogen is bonded to O_1 with a sigma bond, while its interaction with O_2 is charge transfer ($O_2(n_1,n_2)\rightarrow\sigma^*(O_1H)$, whose corresponding energies are 11.15 and 159.30 kcal/mol for n_1 and n_2, respectively). However, the high symmetry of O···H···O, and almost identical natural charges on oxygens (−0.626 and −0.627 for O_1 and O_2, respectively) show that the interactions of hydrogen with the two oxygen atoms must be identical in nature.

In order to determine bonds nature, AIM analysis was carried out for the TS structure of **1b**. For both OH bonds the values of $|V(r)|$ are greater than $G(r)$ and even $2G(r)$, which gives rise to negative values for $H(r)$ and $\nabla^2\rho(r)$ (Table 3). But taking a look at the contour plot of the Laplacian distribution in molecular plane of the TS (Fig. 5) reveals that the hydrogen atom is completely surrounded by a positive area, which means that the valence shell charge concentration (VSCC) of the

hydrogen atom is completely separated from the VSCCs of the two oxygen atoms. However, the hydrogen VSCC is so polarized towards oxygens that the BCPs are located within it, which implies negative value for Laplacian at the BCPs. Therefore, these OH bonds cannot be considered as strictly covalent bonds.

3.2. π-delocalization effects in the nature of RAHBs

To inspect the effects of π-delocalization, systems with more π-delocalization have been chosen (**2a**, **2b**, and **3**), and nature of the H-bond was studied. It is clear that, as delocalization takes place, some double bond character appears in single bonds and vice versa. Also, increasing in bond order is accompanied with decreasing in bond length and increasing in electron density at the BCP, which can be considered as delocalization criteria. Looking at density values at the BCPs and bond lengths in Table 4, it is realized that π-delocalization is more favor in **2a**, **2b** and **3**, than it is in **1b**. Since, there is more π-delocalization, and therefore, stronger H-bond in **2a**, **2b** and **3**, than **1b**, more H-bond stabilization energy is expected for the former systems (Table 2). Note that both the stabilization energy and $\Delta E_{CT}(O···H)$ have the same trend.
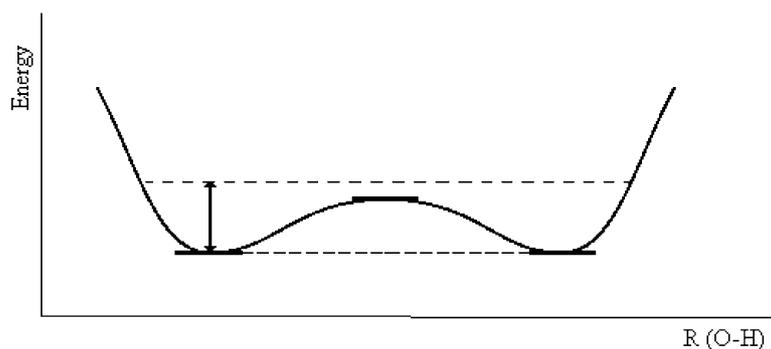
Fig. 4. The classical shape of potential energy surface of hydrogen transfer between oxygens in **1b**. The arrow indicates the ZPE of O–H stretching in local minimum.

Table 3
AIM parameters at the BCPs of OH bonds in the TS structures (B3LYP/6-311 + +G**)

TS	AIM parameters at the BCP of O_1–H bond					AIM parameters at the BCP of O_2–H bond				
	Lap	$\rho(r)$	$G(r)$	$V(r)$	$H(r)$	Lap	$\rho(r)$	$G(r)$	$V(r)$	$H(r)$
1b	−0.304	0.177	0.094	−0.264	−0.170	−0.258	0.172	0.094	−0.253	−0.159
2[a]	−0.303	0.178	0.096	−0.267	−0.171	−0.275	0.175	0.095	−0.259	−0.164
3	−0.322	0.180	0.097	−0.274	−0.177	−0.276	0.176	0.097	−0.263	−0.166
4	−0.304	0.176	0.096	−0.267	−0.172	−0.299	0.176	0.096	−0.266	−0.170
5	−0.336	0.182	0.100	−0.284	−0.184	−0.332	0.181	0.100	−0.283	−0.183
6	−0.278	0.170	0.092	−0.254	−0.162	−0.274	0.170	0.092	−0.253	−0.161

Species **5** is a local minimum.
[a] Transition state between **2a** and **2b**.

Laplacian values for O···H bond in **2a**, **2b** and **3**, are all positive (Table 2), that at first glance seems to be a non-shared interaction. However, as discussed previously, $V(r)$, $G(r)$ and $H(r)$ must be taken into account too. Negative values for $H(r)$, shows some contribution of sharing interaction to the O···H bond, and makes them to be partially covalent. Absolute values of $H(r)$ are increasing from **1b**, **2a**, **2b** to **3**, that shows covalent attribution is enhanced with increasing in π-delocalization. In addition, similar to **1b**, covalent nature of the O–H bond decreases, as it increases in O···H bond for **2a**, **2b** and **3**.

The proton transfer PES for **3** was found as symmetric DM/NB because its ZPE_{O-H} (4.15 kcal/mol in harmonic
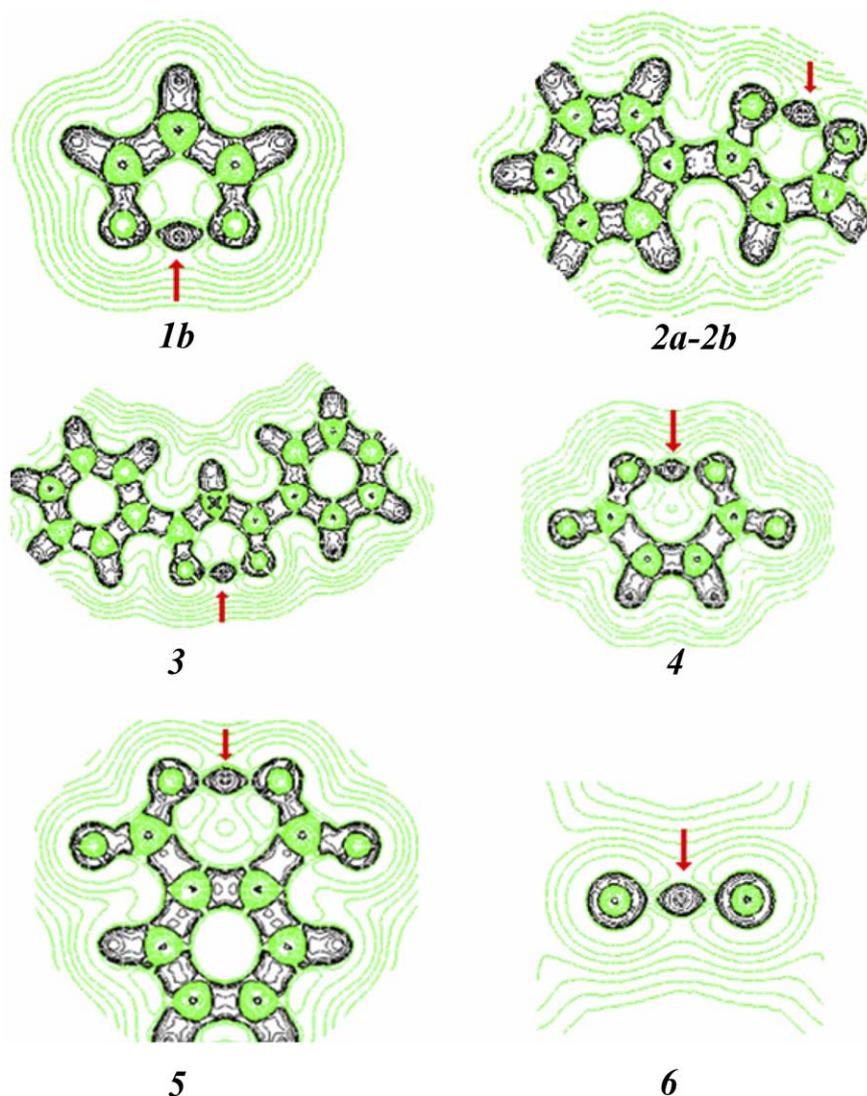
Fig. 5. Contour plot of the Laplacian of the electron density for TS of species (except for **5** which is a local minimum) at B3LYP/6-311 + +G** level. The green and black lines are positive and negative contours, respectively. For **6** only O–H–O part of molecule is shown. Arrows indicate the position of the hydrogen.(For interpretation of the reference to colour in this legend, the reader is referred to the web version of this article)

Table 4
The results of AIM parameters (atomic units) and bond length (Angstrom) for species **1b**, **2a**, **2b** and **3** and their transition state (B3LYP/6-311+ +G**)

Species		O_1–H	O_2···H	O_1–C_1	C_3=O_2	C_2–C_3	C_1=C_2
1b	ρ	0.326	0.049	0.316	0.384	0.289	0.329
	BL	0.998	1.701	1.320	1.238	1.438	1.364
TS of **1b**	ρ	0.177	0.172	0.350	0.352	0.308	0.309
	BL	1.204	1.214	1.279	1.277	1.400	1.398
2a	ρ	0.321	0.055	0.317	0.376	0.283	0.326
	BL	1.001	1.650	1.320	1.250	1.449	1.363
2b	ρ	0.315	0.060	0.314	0.379	0.293	0.317
	BL	1.006	1.613	1.327	1.244	1.429	1.380
TS between **2a** and **2b**	ρ	0.175	0.177	0.350	0.345	0.301	0.311
	BL	1.209	1.201	1.288	1.280	1.395	1.412
3	ρ	0.307	0.068	0.315	0.372	0.287	0.317
	BL	1.011	1.565	1.323	1.255	1.439	1.379
TS of **3**	ρ	0.180	0.175	0.344	0.345	0.303	0.304
	BL	1.196	1.205	1.290	1.289	1.408	1.407

approximation), lies above the barrier (1.81 kcal/mol) between the identical minima. This DM PES converts to a SW shape when ZPC is considered, and perhaps it implies that the hydrogen is not shifting between the two minima. So the nature of bonds in the TS structure is interesting, in which the hydrogen lies nearly at the middle of distance between the two oxygens (Table 4), and there are almost identical charge transfers from both oxygen lone pairs to the n^* of hydrogen (229.62 and 222.68 kcal/mol). At the BCP of two O–H bonds in the TS electron density and $\nabla^2\rho$ have almost identical magnitude too (Table 3). The sign of $\nabla^2\rho(r)$ and $H(r)$ for these bonds suggest a covalent nature, however, positive areas between the VSCCs of oxygens and hydrogen in the contour plot of the $\nabla^2\rho$ (Fig. 5) indicates some contribution of closed-shell (electrostatic) interaction to these bonds.

Structures **2a** and **2b** are two different minima, belong to one PES with the corresponding $ZPE_{O–H}=4.44$ and 4.30 kcal/mol, for **2a** and **2b**, respectively, and both of them are above the barrier. Therefore, an asymmetric DM/NB PES is obtained which is converted to a SW shape after considering ZPC. For TS in this PES, the same explanation for O–H bonds as **1b** and **3** exists (Table 3), that is both OH bonds are covalent with some electrostatic contribution.

3.3. Chemical nature of (±)CAHBs

As it was introduced, very strong hydrogen bonds can be occurred in either RAHB or (±)CAHB. In (+)CAHBs, the molecular charge is positive, but it is negative for (−)CAHBs. In this part, we are going to study the nature of H-bond in **4**, **5** and **6** (Fig. 1) in which their very strong H-bond detected experimentally [19]. The hydrogen bonds in **4** and **5** are intramolecular (−)CAHB, while, it is an intermolecular (+)CAHB in **6**.

All efforts to calculate the H-bond energy in **4** (and **5**) has been failed. Because, to make open systems, rotation of O_1–H bond about C_1–O_1 in **4** (and **5**), substitutes the O_2···H bond with a new H-bond between O_3 and the hydrogen. This new H-bond causes preventing a molecule without hydrogen bond

in a particular position of molecule. Consequently, the stabilization energy, which is the energy difference between molecule with and without hydrogen bond, cannot be obtained. Therefore, it is preferred to find out about the strength hydrogen bond in these species indirectly, which are the interpretation of NBO and AIM analysis as before.

The sum of charge transfer energies from O_2 lone pair (n_1 and n_2) to the σ^* of O_1–H in **4** (Table 2), is 113.6 kcal/mol, which is considerably larger than **1b**, **2a**, **2b** and **3**. According to Ref. [45] which states that "strong CT tends to shorten and strengthen O···H bonds", one may find that the hydrogen bond in **4** must be stronger than those of **1b**, **2a**, **2b** and **3**. On the other hand, AIM electron densities also confirm this conclusion; the electron density in BCP on O···H bond is larger for **4** in comparison to **1b**, **2a**, **2b** and **3** as shown in Table 2.

The nature of hydrogen bond (O_2···H) in **4** can be understood from four AIM values of $\nabla^2\rho(r)$, $G(r)$, $V(r)$ and $H(r)$ at the BCP, as previously discussed for **1b**, and the results for this case presented in Table 2. According to these values, we suggest, this H-bond to be partially covalent and partially electrostatic. This is against the electrostatic character predicted by Lluch et al. [25], which was justified entirely by sign of $\nabla^2\rho(r)$.

A symmetric transition state for hydrogen transfers between two oxygen atoms on PES for compound **4** has also been obtained with an imaginary frequency about 440.74 cm^{-1}. The barrier for such proton transfer was very small (0.08 kcal/mol), which considerably lies below the $ZPE_{O–H}$ (2.20 kcal/mol). When ZPC was considered, this DM/NB PES converted to SW type. The bond lengths of O_1H and O_2H at TS are almost identical (1.200 and 1.199 Å). In NBO point of view, one of these bonds is indicated by a sigma bond while the other is completely formed by charge transfer from oxygen lone pairs (n_1 and n_2) to $\sigma^*_{O–H}$ which their corresponding energies are 12.06 and 173.72 kcal/mol, respectively. The equal natural charges on the both oxygens (−0.733) and also identical BCP properties for these bonds (Table 3) confirm that these two O–H bonds are identical in nature.

Geometry of hydrogen phthalate anion (**5**), as another case for (−)CAHBs, have been also optimized. In agreement with Lluch et al. [26], a unique stationary point with no imaginary frequency was found, which corresponds to a potential energy minimum with a symmetric intramolecular hydrogen bond located at a symmetric SW/NB PES. In NBO point of view, formation of both O–H bonds is accompanied with a large charge transfer from the two oxygen lone pairs into the hydrogen Rydberg orbitals (238.86 and 238.95 kcal/mol). Electron densities at the BCPs of both O–H bonds (Table 2) lie between what is expected for an ordinary O–H covalent bond and O···H hydrogen bond that shows how 3-center 4-electron it is. The negative sign of $\nabla^2\rho(r)$ and $H(r)$ at the BCPs of these two bonds, proposed covalent character for them, however, the separations between VSCC of hydrogen and oxygen atoms in the contour plot of $\nabla^2\rho$ (Fig. 5), indicate that electrostatic interactions have some contributions to these
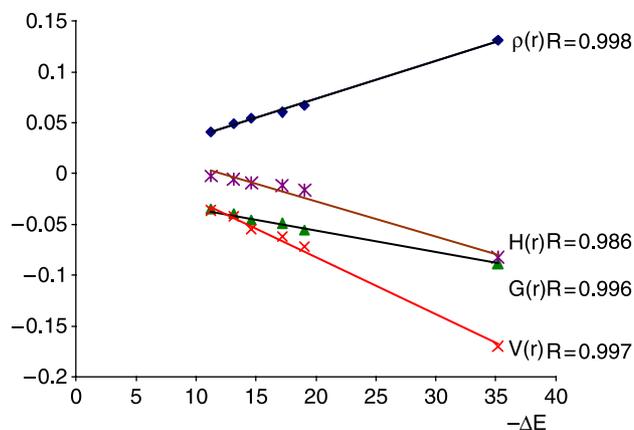
Fig. 6. Correlation of O···H AIM parameters with H-bond energy. Horizontal axis is H-bond energy in kilocalorie per mole, and vertical axis is related to different AIM parameters in atomic units. 'R' is correlation coefficient.

bonds, similar to those that was obtained for O–H bonds in TSs of previous species.

The last case, which has been studied, is an intermolecular hydrogen bond between methylsulfinylmethane and its corresponding protonated cation (6 in Fig. 1). The calculated stabilization energy due to the H-bond, was about 35.2 kcal/mol, which lies in the very strong hydrogen bond region and can be classified as (+)CAHBs. A structure with a near to zero imaginary frequency (45 cm^{-1} in harmonic approximation) has been detected at the middle of its symmetric DM/NB type profile, which lies only 0.02 kcal/mol above the two minima. This barrier is too small to have practical physical meaning and vanishes when ZPC is considered. The sign of $\nabla^2\rho(r)$ and $H(r)$ and the value of $\rho(r)$ at the BCPs of OH bonds in this stationary state, suggests share (covalent) interactions between hydrogen and oxygen atoms. However, the contour plot of $\nabla^2\rho(r)$ for O–H–O part shows that VSCC of the bridge hydrogen is well separated from those of oxygen atoms (Fig. 5), which means that, OH interactions are not purely covalent.

In the local minimum of 6, strong charge transfers from lone pairs of oxygen atom, which accepts the H-bond, into the σ_{OH}^*,

tends to lengthen (and weaken) the O–H segment and to shorten (and strengthen) the O···H bond (Table 2). The AIM parameters for O···H bond (Table 2), show that it is not purely electrostatic and covalent character has been considerably contributed to this bond.

3.4. Overview

With respect to parameters in Table 2, there is a correlation between the H-bond energy and $\rho(r)$, $G(r)$, $V(r)$ and $H(r)$ for both O–H and O···H bonds in the investigated spices. The linear dependency between H-bond energy and the above parameters at the BCP of O···H bonds is shown in Fig. 6. Using the relationship between $\rho(r)$ and ΔE_{HB}, H-bond energy for 4 and 5 was extracted as 33.7 and 49.4 kcal/mol, respectively. In addition, it is clear from Fig. 6, that as the H-bond energy and $\rho(r)$ at the BCP of O···H increases the absolute value of $H(r)$ and hence the covalent nature of O···H bond increase too. Furthermore, a desirable trend was found between ΔE_{HB} and $\nabla^2\rho(r)$ in RAHBs, however, ($\pm$)CHABs species do not follow this trend.

Although for all species the ratio of $G(r)/\rho(r)$ for O···H is less than one, no trend have been observed for this quantity with the other parameters in Table 2. In addition, these ratios are close to those that were obtained for hydrogen bond in water dimmer (at the same level of calculation, is about 0.84), which indicates this is not a good quantity to distinguish between different H-bond types.

Furthermore, it is clear from Table 2 that, as the O–H–O angle in intramolecular H-Bonds (1b, 2a, 2b, 3 and 4) approaches to 180°, and O···O separation decreases, the charge transfers from oxygen lone pairs (n_1 and n_2) to $\sigma_{O_1H}^*$ increase, although, this increase is more significant for n_1, which is aligned toward O_1–H bond and hence its σ^* NBO (for example see Fig. 3 for 1b).

As mentioned before, all of above results has been obtained with B3LYP functional, a theory that is valuable because of its computational efficiency. In order to demonstrate the ability of this method for description of PESs and O–H bond natures, an MP2/6-311++G** calculation has been done for 1b, 2a, 2b, 4 and 6. The results are summarized in Tables 5 and 6. It seems

Table 5

Barrier of proton transfers, PES shapes, AIM parameters and geometries of species in their local minimum (MP2/6-311++G**)

	ΔE_{PT}[a]	PES	AIM parameters at the BCP of O–H bond					AIM parameters at the BCP of O···H bond					Geometries of O–H···O part			
			ρ [−1]	Lap	$G(r)$ [−2]	$V(r)$ [−1]	$H(r)$ [−1]	ρ [−2]	Lap [−1]	$G(r)$ [−2]	$V(r)$ [−2]	$H(r)$ [−2]	Distances			Angle
													O–H	O···H	O···O	
1b	3.27	DM/NB-DW	3.27	−2.307	7.14	−7.20	−6.48	4.89	1.37	4.16	4.88	−0.70	0.991	1.694	2.589	148.2
2a	2.89	DM/NB-SW	3.21	−2.240	7.28	−7.05	−6.33	5.58	1.49	4.80	5.90	−1.09	0.997	1.639	2.544	148.8
2b	2.45	DM/NB-SW	3.16	−2.180	7.39	−6.93	−6.19	6.00	1.51	5.11	−6.46	−1.34	1.001	1.609	2.536	151.9
4	0.046	DM/NB-SW	2.26	−0.998	9.47	−4.39	−3.44	13.1	0.29	9.38	−18.0	−8.66	1.106	1.300	2.406	179.3
6	0.037	DM/NB-SW	2.18	−0.943	9.21	−4.20	−3.28	12.8	0.37	9.28	−17.6	−8.34	1.109	1.292	2.400	176.6

[a] Proton transfers barriers in kilocalorie per mole.

Table 6
AIM parameters at the BCPs of OH bonds in the TS structures (MP2/6-311++G**)

TS	AIM parameters at the BCP of O_1–H bond					AIM parameters at the BCP of O_2–H bond				
	Lap	$\rho(r)$	$G(r)$	$V(r)$	$H(r)$	Lap	$\rho(r)$	$G(r)$	$V(r)$	$H(r)$
1b	−0.325	0.177	0.101	−0.283	−0.182	−0.317	0.177	0.101	−0.281	−0.180
2	−0.340	0.179	0.101	−0.288	−0.187	−0.311	0.176	0.101	−0.281	−0.179
4	−0.340	0.176	0.101	−0.287	−0.186	−0.334	0.176	0.101	−0.285	−0.184
6	−0.319	0.171	0.098	−0.276	−0.178	−0.312	0.170	0.098	−0.274	−0.176

that in most aspects, MP2 reproduces the B3LYP results; The shape of PESs are similar to what was obtained at DFT calculation, and the AIM parameters indicate that hydrogen bonds in the minima of this species can be characterized as partially covalent and partially electrostatic. The main difference between the results are related to the contour plot of the Laplacian of the electron densities of the some species in their TS; although B3LYP show that the VSCC of hydrogen atoms in the TS of **1b**, **2a-2b** and **4**, are well separated from those of oxygen atoms, MP2 wave functions indicate a continuous region between VSCC of hydrogen and oxygen atoms (Fig. 7). This means that MP2 calculations predict two identical covalent hydrogen bonds in the TSs of these compounds. As it clear from Fig. 7, there is no significant difference between the results of B3LYP and MP2 for the TS of **6**.

4. Conclusion

A topological analysis of electron density of RAHBs and (±)CAHBs at B3LYP/6-311++G** level of theory, indicates that these hydrogen bonds are partially covalent. The covalent character of H-bond, with the criterion of absolute value of $H(r)$, is increased with π-delocalization and is proportional to stabilization energy and charge transfer from oxygen lone pairs to anti bonding NBO of O–H. From Table 2, an acceptable correlation can be seen in $H(r)$ vs. $\rho(r)$ and 'H-bond energy' vs. $\rho(r)$. Also, it is revealed that the covalent

character of O···H bond increases as this character decreases for O–H bond.

All PES for investigated systems, was found as DM/NB type with regards to O–H···O stretching frequencies and their corresponding barrier, which decreases with more π-delocalization in RAHBs. Since, in their TS, the hydrogen atom is located nearly at the middle of O···O separation, and both AIM and NBO results show the same character for both O–H bonds, a 3-center 4-electron bond is expected. Although $\nabla^2\rho$ and $H(r)$ are negative at the two O–H BCPs (Table 3), indicating covalent nature, the VSCC of the hydrogen atom is well separated from that of oxygens (Fig. 5), indicating the contribution of electrostatic interaction.

MP2/6-311++G** calculations for **1b**, **2a**, **2b**, **4** and **6**, are also reproduce the above results for the nature of hydrogen bonds and the shape of PESs. For TSs of **1b**, **2a-2b** and **4**, MP2 shows a continuous region of space between hydrogen and oxygen atoms, over which the $\nabla^2\rho(r)$ is negative.

References

[1] M.L. Huggins, Thesis, University of California, 1919.
[2] W.M. Latimer, W.H. Rodebush, J. Am. Chem. Soc. 42 (1920) 1419.
[3] G.N. Lewis, Valence and the structure of atoms and molecules, New York: The Chemical Catalog Company, 1923.
[4] G.C. Pimentel, A.L. McClellan, The Hydrogen Bond, San Francisco, CA: Freeman, 1960.
[5] W.C. Hamilton, J.A. Ibers, Hydrogen Bonding in Solids, New York: Benjamin, 1968.
[6] P. Schuster, G. Zundel, C. Sandorfy (Eds.) The hydrogen bond. Recent developments in theory and experiments, Vol. I, II and III, Amsterdam: North-Holland Publication Company, 1976.
[7] G.A. Jeffrey, W. Saenger, Hydrogen bonding in biological structures, Berlin: Springer, 1991.
[8] G.A. Jeffrey, An Introduction to hydrogen Bonding, New York: Oxford University Press, 1997.
[9] G.R. Desiraju, T. Steiner, The week hydrogen bond in structural chemistry and biology, New York: Oxford University Press, 1999.
[10] G.C. Pimentel, A.L. McClellan, Annu. Rev. Phys. Chem. 22 (1971) 347.
[11] P.A. Kollman, L.C. Allen, Chem. Rev. 72 (1972) 283.
[12] W.W. Cleland, M.M. Kreevoy, Science 264 (1994) 1887.
[13] P.A. Frey, S.A. Whitt, J.B. Tobin, Science 264 (1994) 1927.
[14] A. Warshel, A. Papazyan, P.A. Kollman, Science 269 (1995) 102.
[15] S. Vishveshwara, M.S. Madhusudhan, J.V. Maizel Jr., Biophys. Chem. 89 (2001) 105.
[16] G. Gilli, F. Bellucci, V. Ferretti, V. Bertolasi, J. Am. Chem. Soc. 111 (1989) 1023.
[17] V. Bertolasi, P. Gilli, V. Ferretti, G. Gilli, J. Am. Chem. Soc. 113 (1991) 4917.
[18] G. Gilli, V. Bertolasi, V. Ferretti, P. Gilli, Acta Crystallogr B49 (1993) 564.
[19] P. Gilli, V. Bertolasi, V. Ferretti, G. Gilli, J. Am. Chem. Soc. 116 (1994) 909.
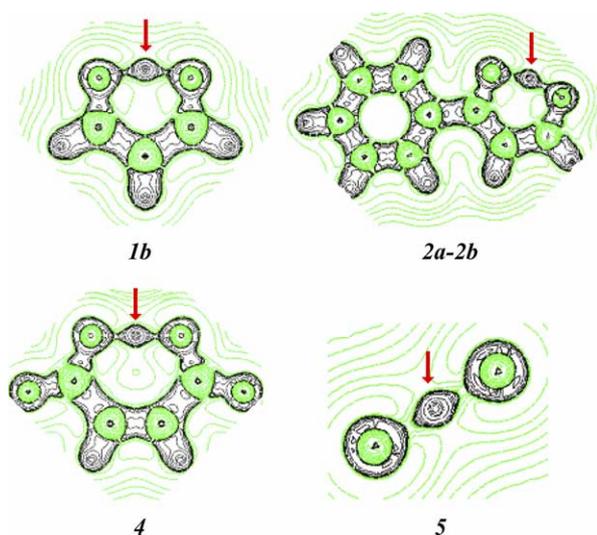
Fig. 7. Contour plot of the Laplacian of the electron density for TS of some species at MP2/6-311++G** level of theory.

[20] G. Gilli, P. Gilli, J. Mol. Struct. 552 (2000) 1.
[21] P. Gilli, V. Bertolasi, V. Ferretti, G. Gilli, J. Am. Chem. Soc. 122 (2000) 10405.
[22] P. Gilli, V. Bertolasi, L. Pretto, A. Lyčka,, G. Gilli, J. Am. Chem. Soc. 124 (2002) 13554.
[23] P. Gilli, V. Bertolasi, L. Pretto, V. Ferretti, G. Gilli, J. Am. Chem. Soc. 126 (2004) 3845.
[24] P. Gilli, V. Bertolasi, L. Ferretti, L. Antonov, G. Gilli, J. Am. Chem. Soc. 127 (2005) 4943.
[25] M.G. Viloca, A.G. Lafont, J.M. Lluch, J. Am. Chem. Soc. 119 (1997) 1081.
[26] M.G. Viloca, A.G. Lafont, J.M. Lluch, J. Am. Chem. Soc. 121 (1999) 9198.
[27] S. Wojtulewski, S.J. Grabowski, J. Mol. Struct. (Theochem) 621 (2003) 285.
[28] A. Mohajeri, J. Mole. Struct. (Theochem) 678 (2004) 201.
[29] F. Hibbert, J. Emsley, Adv. Phys. Org. Chem. 26 (1990) 255.
[30] G.K.H. Madsen, B.B. Iversen, F.K. Larsen, M. Kapon, G.M. Reisner, F.H. Hrbstein, J. Am. Chem. Soc. 120 (1998) 10040.
[31] B. Schiøtt, B.B. Iversen, G.K.H. Madsen, T.C. Bruice, J. Am. Chem. Soc. 120 (1998) 12117.
[32] R.F.W. Bader, Atoms in molecules: a quantum theory, Oxford, UK: Oxford University Press, 1990.
[33] A.E. Reed, L.A. Curtiss, F. Weinhold, Chem. Rev. 88 (1988) 899.
[34] F. Weinhold, Natural bond orbital methods in: P.v.R. Schleyer (Ed.), Encyclopedia Comput. Chem., Wiley, Chichester, UK, 1998, pp. 1793–1810.
[35] M.J. Frisch, G.W. Trucks, H.B. Schlegel, G.E. Scuseria, M.A. Robb, J.R. Cheeseman, V.G. Zakrzewski, J.A. Montgomery, Jr., R.E. Stratmann, J.C. Burant, S. Dapprich, J.M. Millam, A.D. Daniels, K.N. Kudin, M.C. Strain, O. Farkas, J. Tomasi, V. Barone, M. Cossi, R. Cammi, B. Mennucci, C. Pomelli, C. Adamo, S. Clifford, J. Ochterski, G.A. Petersson, P.Y. Ayala, Q. Cui, K. Morokuma, D.K. Malick, A.D. Rabuck, K. Raghavachari, J.B. Foresman, J. Cioslowski, J.V. Ortiz, B.B. Stefanov, G. Liu, A. Liashenko, P. Piskorz, I. Komaromi, R. Gomperts, R.L. Martin, D.J. Fox, T. Keith, M.A. Al-Laham, C.Y. Peng, A. Nanayakkara, C. Gonzalez, M. Challacombe, P.M.W. Gill, B. Johnson, W. Chen, M.W. Wong, J.L. Andres, C. Gonzalez, M. Head-Gordon, E.S. Replogle, J.A. Pople, GAUSSIAN 98, Revision A.7, Pittsburgh PA: Gaussian, Inc., 1998.
[36] A.D. Becke, J. Chem. Phys. 98 (1993) 5648.
[37] C. Lee, W. Yang, R.G. Parr, Phys. Rev. B37 (1988) 785.
[38] E.D. Glendening, A.E. Reed, J.E. Carpenter, F. Weinhold, NBO Version 3.1.
[39] R.F. W. Bader, AIM2000 Program Package, Ver. 2.0, Hamilton, Ont.: McMaster University, 2002.
[40] J. Emsley, Struct. Bonding 57 (1984) 147.
[41] S.J. Grabowski, J. Phys. Chem. A 105 (2001) 10739.
[42] S.J. Grabowski, Monatshefte für Chemie 133 (2002) 1373.
[43] F. Weinhold, J. Mol. Struct. (Theochem) 398-399 (1997) 181.
[44] A.E. Reed, F. Weinhold, J. Chem. Phys. 83 (1985) 1736.
[45] R.W.F. Bader, J. Phys. Chem. A 102 (1998) 7314.
[46] D. Cremer, E. Kraka, Angew. Chem. 23 (1984) 627.
[47] S. Jenkins, I. Morrison, Chem. Phys. Lett. 317 (2000) 97.
[48] T.S. Koritsanszky, P. Coppens, Chem. Rev. 101 (2001) 1583.
[49] P. Popelier, Atoms in molecules, an Introduction, Prentice-Hall, Pearson Education Limited, 2000.
[50] R. Bianchi, G. Gervasio, D. Marabello, Inorg. Chem. 39 (2000) 2360.